

The fracture and fragmentation behaviour of additively manufactured stainless steel 316L

Cite as: AIP Conference Proceedings **1793**, 100002 (2017); <https://doi.org/10.1063/1.4971627>
Published Online: 13 January 2017

R. Amott, E. J. Harris, R. E. Winter, S. M. Stirk, D. J. Chapman, and D. E. Eakins



View Online



Export Citation

ARTICLES YOU MAY BE INTERESTED IN

[On the dynamic response of additively manufactured 316L](#)

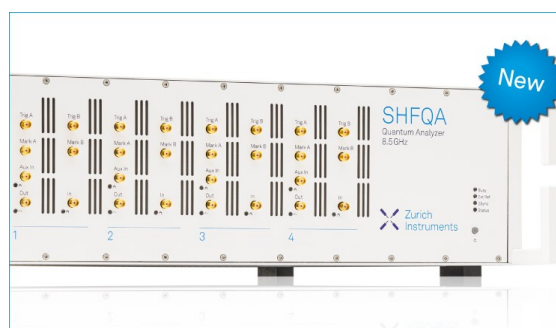
AIP Conference Proceedings **1799**, 060007 (2018); <https://doi.org/10.1063/1.5044804>

[A gas gun based technique for studying the role of temperature in dynamic fracture and fragmentation](#)

Journal of Applied Physics **114**, 173508 (2013); <https://doi.org/10.1063/1.4828867>

[Spall fracture in additive manufactured Ti-6Al-4V](#)

Journal of Applied Physics **120**, 135902 (2016); <https://doi.org/10.1063/1.4963279>



Your Qubits. Measured.

Meet the next generation of quantum analyzers

- Readout for up to 64 qubits
- Operation at up to 8.5 GHz, mixer-calibration-free
- Signal optimization with minimal latency

Find out more



The Fracture and Fragmentation Behaviour of Additively Manufactured Stainless Steel 316L

R. Amott ^{1,a)}, E. J. Harris ¹, R. E. Winter ¹, S. M. Stirk ¹, D. J. Chapman ² and D. E. Eakins ²

¹*AWE, Aldermaston, Reading, RG7 4PR, United Kingdom*

²*Institute of Shock Physics, Imperial College London, Prince Consort Road, London, SW7 2AZ, United Kingdom*

a) Russell.Amott@awe.co.uk

Abstract. Expanding cylinder experiments using a gas gun technique allow investigations into the ductility of metals and the fracture and fragmentation mechanisms that occur during rapid tensile failure. These experiments allow the radial strain-rate of the expansion to be varied in the range 10^2 to 10^4 s⁻¹. Presented here is a comparative study of the fracture and fragmentation behaviour of rapidly expanded stainless steel 316L cylinders manufactured from either a wrought bar or additive manufacturing techniques. The results show that in the strain-rate regime studied, an additively manufactured cylinder failed at a higher strain and produced larger fragment widths when compared to cylinders manufactured from a wrought bar. In addition, an investigation into the role of macroscopic elongated voids that were introduced into the cylinder wall, at an angle of 45° to the cylinder radius, was undertaken. A comparison between experimental and simulated results (using the Eulerian hydrocode CTH) was also completed.

INTRODUCTION

Some of the most interesting properties of a material come to light when observing how it fails under high rate tensile loading. A number of different experimental techniques exist to generate failure under dynamic tensile loading, with large volumes of work focused on the expansion of cylinders. Expanding cylinder experiments can be modified to generate large or small radial strain-rates under multiple loading conditions, enabling investigations into the fracture and fragmentation mechanisms within a variety of different materials. A non-explosive method was pioneered by Winter et al. ¹ in the 1970's by adapting gas guns, which were predominantly used for plate impact studies, to expand cylinders. Winter partially filled a cylinder with a rubber silastomer before impacting it with a nylon projectile, imparting the projectile's momentum into the rubber infill and subsequently expanding the cylinder to failure. This method of loading generated radial strain-rates of 10^4 s⁻¹ by providing a continuous mechanical drive to expand the cylinders to failure. However, the temporal history of expansion was complex as the stress-strain relationship was neither uniaxial nor truly biaxial. This coupled with the fact that the peak in cylinder expansion was seen to translate along the axis, a consequence of momentum transfer in the impact direction, made analysis of these events difficult. Vogler et al. ² improved on the Winter method by replacing the silastomer and nylon with polycarbonate, which produced a more symmetric expansion around the impact plane. This configuration, which was adapted for the present study, was successful at reducing the observed translation whilst still reaching radial strain-rates of interest.

Additive manufacturing (AM) and more specifically Selective Laser Melting (SLM) allows 3D samples to be created by fusing small particulates together with a high powered laser. A design is fed into the additive machine and after one layer or cross section has been fused, the assembly moves down one step before another layer of powder is applied and the process is repeated. One of the advantages of this manufacturing method is that novel structures can be created that conventional manufacturing methods could not achieve. Material properties are known

to differ between additive and conventionally manufactured samples with little in the literature on the dynamic failure of AM materials. Cylinders of stainless steel 316L, manufactured by additive and conventional techniques, were expanded and compared with each other using the large bore gas gun at the Institute of Shock Physics (ISP), Imperial College London. AM methods were also used to introduce deliberate defects into a cylinder wall before expansion to understand failure mechanisms by controlling the location and orientation of shear fractures.

EXPERIMENTAL METHOD

A stainless steel 316L cylinder 170 mm in length, with an outer diameter of 72.8 mm and wall thickness of 1.5 mm was filled with a polycarbonate infill to a length of 85 mm. The cylinder and infill were attached to an end cap (used to aid the assembly process) using a low viscosity epoxy with a 40 mm long chamfer machined onto the cylinder's inner wall. For alignment purposes a mount held the entire assembly in place with six grub screws used to make any adjustments to the position of the cylinder relative to the barrel of the gun. Two metal arms were then attached to the main cylinder mount to enable the fielding of laser diagnostics; the projectile was 235 mm in length with the final assembly shown in Fig. 1.

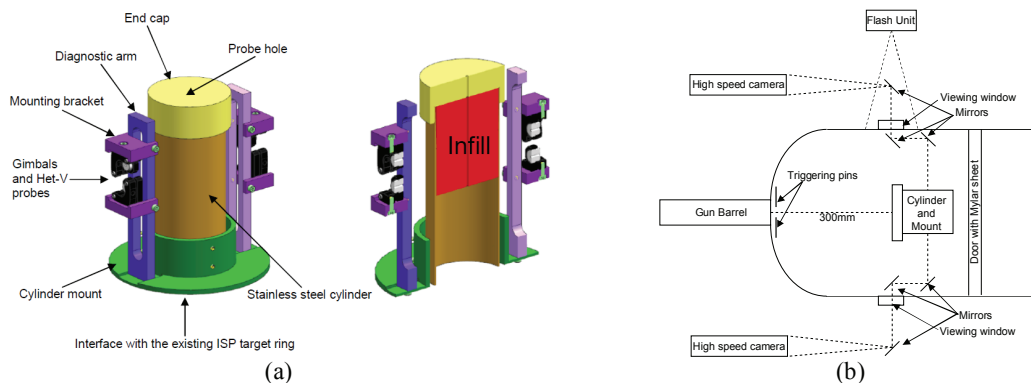


FIGURE 1. (a) The final assembly (left) with the cylinder in brown, cylinder mounts in green, mounting brackets and diagnostic arms in purple, end cap in yellow and the gimbals in black. The section view (right) shows the polycarbonate infill within the cylinder in red. (b) Shows the cylinder assembly inside the facilities at the ISP (viewed from above and not to scale).

Radial expansion velocities were measured using Heterodyne Velocimetry (Het-V) ³, mounted on a diagnostic arm that could field multiple fibre probes on each shot. Two focusing fibres on each diagnostic arm were used to measure the radial velocity of the cylinder (frequency shifted) at different points along its length. A collimating probe, located within the infill and flush to the impact face, measured impact velocity of the projectile. Kinematic mounts housed each focusing fibre and were attached via a mounting bracket to the diagnostic arm. The target tank at the ISP included three viewing ports which were used to introduce light to the target cylinder and also allow the fielding of two high speed cameras on each shot. Three different cameras were used in total; a Phantom V1610, V2010 and Invisible Vision Ultra UHSi 12/24 high-speed framing camera to record the temporal history of the cylinder. These images were then used to calculate the peak strain experienced at first crack appearance (signifying that failure had occurred).

RESULTS AND DISCUSSION

Four expanding cylinder experiments were completed (two AM and two manufactured from a wrought bar) with samples taken before firing for imaging with optical microscopy and Electron Back Scatter Diffraction (EBSD). A selection of these images is shown in Fig 2. Previous studies on the microstructure of AM materials ⁴ had suggested that the build direction, laser speed and hatching arrangement (variables in the SLM process) would all determine not only the final part density but also the grain size, structure and orientation. The average grain size for the AM sample was $21 \pm 6 \mu\text{m}$ and anisotropic (elongated in the build direction) whilst the conventional sample was $13 \pm 3 \mu\text{m}$ and equi-axed. This anisotropy in AM samples has been noted by others ⁵ and is likely due to the large thermal gradients that are set up during the build process when melt pools form and preferentially orientate as they cool.

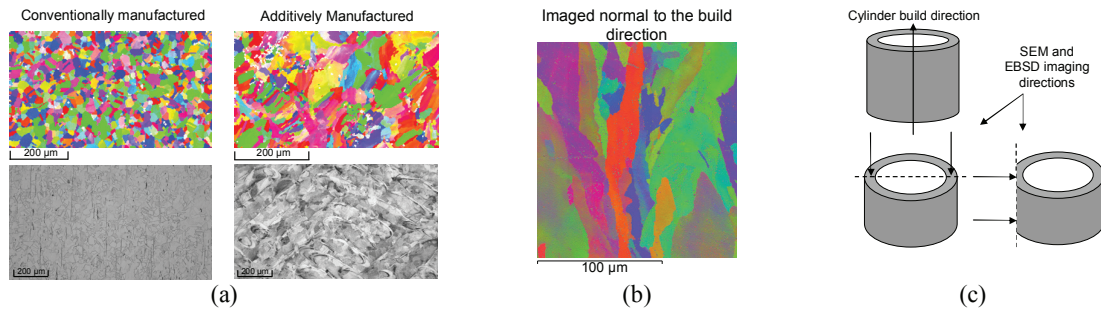


FIGURE 2. (a) EBSD (top) gave the grain size whilst (bottom) optical microscopy imaged the melt pools and annealing twins. (b) EBSD imaged in a direction normal to the AM cylinders build direction highlighting the anisotropy in grain orientation (with respect to grain morphology). (c) Shows the different imaging directions that were used.

Results from AM cylinders are shown in Fig 3. and Fig 4. alongside simulations completed using the Eulerian hydrocode CTH. Reasonable agreement was found between Het-V (corrected for impact time) and simulation, except for a number of small oscillations (probably due to the tight tolerance between cylinder and projectile) and late time features that were predicted by the code and not seen experimentally.

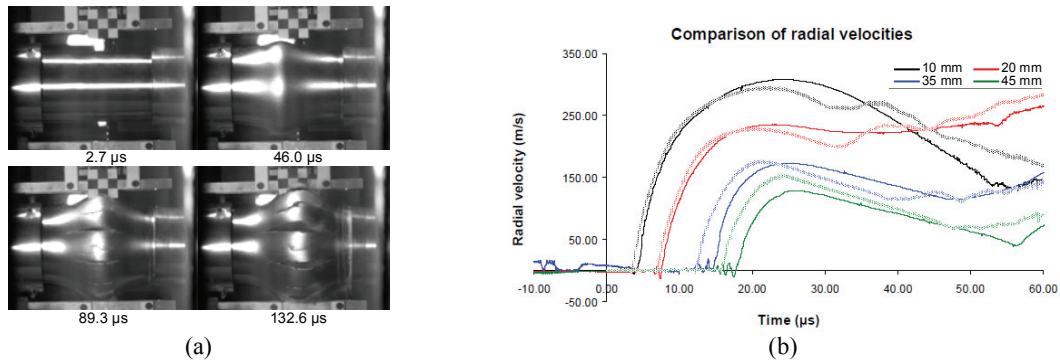


FIGURE 3. (a) Images from a V1610 camera showing the expansion of an AM cylinder without intentional defects, times are given with respect to impact time. The projectile enters from the left with expansion around the midpoint; longitudinal cracks are visible by the third image. (b) Comparison between experimental (solid) and simulated (hatched) radial velocities, with each trace representing a different distance from the impact plane. The simulations used a Mie-Gruneisen EoS a Mulliken-Boyce strength model (for polycarbonate) ⁶ and a Steinburg strength model (with a modified yield strength of 0.64 GPa for AM SS316L) ⁷.

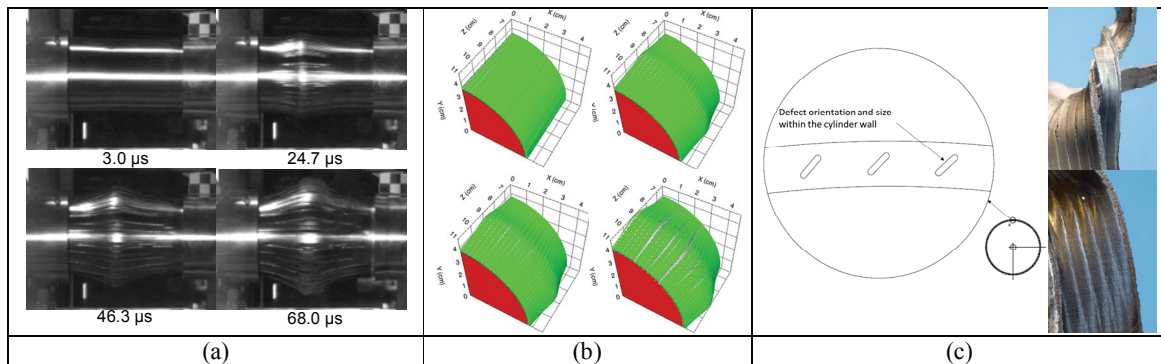


FIGURE 4. (a) Images taken by a Phantom V1610 camera showing the expansion and failure of an AM stainless steel cylinder which included defects seeded during the build process; times are given with respect to impact time. The projectile enters from the left with expansion around the midpoint; shear localization can be seen as striations along the cylinders length. (b) 3D simulations completed in CTH. (c) Images of recovered fragments showing strain localization along the defect plane.

Figure 4 shows the expansion of an AM cylinder which included 100 defects (areas of un-melted powder, 0.7 mm in length, 0.2 mm wide and angled at 45° to the inner surface) left during the build process. These results are markedly different to those in Fig 3. Strain was localized at each defect location and was seen as striations along the cylinders length in the high speed images. The STL file, used to manufacture the cylinder, was also used as an input deck for 3D simulations in CTH which were able to replicate the striations with a calculated inter crack spacing of 7.7 mm compared with an experimental value of 12.7 mm. Control over the orientation of each failure site (all in the same direction) was achieved via the introduction of these defects but at the cost of ductility. A summary of the results from the series is shown in Table 1. Fragmentation toughness (as described by Grady⁸) has been included for comparative purposes as a value could not be found in the open literature for stainless steel 316L.

TABLE 1. Key results from the series

Cylinder	Impact velocity (m/s)	Strain-to-failure (%)	Average radial strain-rate (s ⁻¹)	Average fragment width (mm)	Fragmentation toughness (MPa m ^{1/2})
AM without defects	682.6 ± 1.0	35 ± 3	7.8 x 10 ³	19.2 ± 1.6	230
AM with defects	735.5 ± 1.5	20 ± 3	9.4 x 10 ³	12.7 ± 0.7	
Conventionally manufactured	735.3 ± 1.1	19 ± 2	8.2 x 10 ³	16.4 ± 1.2	219
Conventional manufactured	741.1 ± 1.2	23 ± 2	8.5 x 10 ³	15.3 ± 1.0	

CONCLUSIONS AND FUTURE WORK

Four cylinders of stainless steel 316L were expanded to failure, values of strain-to-failure (a measure of ductility) showed that the AM cylinder was more ductile than its conventionally manufactured counterpart. It is proposed that this change in ductility was due to the preferential orientation of the grains that were generated during the AM build process. Control over the orientation of failure sites was achieved via the introduction of macroscopic defects into the cylinder wall but at a cost of overall material strength and ductility. Fragments from each experiment were collected, but a soft recovery technique will need to be used in the future if changes in the microstructure are to be understood. Simulations using the hydrocode CTH showed reasonable correlation at early time but as failure began, a departure from experimental data was observed. Future work should focus on the effect AM has on a material's final microstructure as it appears to play an important role in the mechanisms of failure. The introduction of different sized defects using additive techniques could enable an understanding into how fracture patterns relate to a material's defect distribution. Multiple impact velocities should be used so that the effect of strain-rate on ductility can be understood; possibly leading to the development of a strain-rate dependant failure model. Expansion of rings rather than cylinders would mean that a condition of uniaxial stress would be maintained throughout the experiment resulting in a simpler interpretation of the data.

ACKNOWLEDGMENTS

The authors would like to acknowledge and thank Dr D. Jones, Mr S. Johnson and Mr D. Pitman from Imperial College London and Miss K. Smith, Dr. P. Ryan, Mr A. Smith and Mr J. Brigden from AWE. The Institute of Shock Physics acknowledges its continued support from AWE and Imperial College London.

REFERENCES

1. R. E. Winter, "Measurement of fracture strain at high strain rates." In Proc. 2nd Conf. Mechanical Properties of Materials at High Rates of Strain, Oxford, England, Mar. 1979, pp. 81-89. 1980.
2. T. J. Vogler et al. [International journal of impact engineering](#) **29**, 735-746 (2003).
3. O. T. Strand et al. [Review of Scientific Instruments](#) **77**, 083108 (2006).
4. L. Thijs et al. [Acta Materialia](#) **58**, 3303-3312 (2010).
5. T. Niendorf et al. [Advanced Engineering Materials](#) **16**, 857-861 (2014).

6. A. D. Mulliken and M. C. Boyce, "Mechanics of the rate-dependent elastic-plastic deformation of glassy polymers from low to high strain rates" [Int. J. Solids Struct.](#) **43** pp.1331-1356 (2006)
7. D. J. Steinberg, "Equation of state and strength properties of selected materials, Lawrence Livermore National Laboratory report UCRL-MA-106439 (1991)
8. D. Grady, *Fragmentation of rings and shells: the legacy of NF Mott*. Springer Science & Business Media 2007.